

# Modelling and Estimation of Sea-Ice Reflectivity: MOSAiC Results on GNSS Reflectometry

M. Semmling (1), J. Wickert (2,3), M. Hoque (1), D. Divine (4), S. Gerland (4), G. Spreen (5)

(1) German Aerospace Centre, Institute for Solar-Terrestrial Physics (DLR-SO)

(2) German Research Centre for Geosciences (GFZ)

(3) Technische Universität Berlin, Institute of Geodesy and Geoinformation Science

(4) Norwegian Polar Institute (NPI), Fram Centre

(5) University of Bremen, Institute of Environmental Physics



## Abstract

The L-band signals transmitted by Global Navigation Satellite Systems (GNSS) are a promising source for sea-ice remote sensing as they partly penetrate into ice upon reflection. Reflecting interfaces of sea-ice layer and snow cover contribute to the reflected signal. We present calculations of sea-ice reflectivity for GNSS signals based on a multilayer reflection model. Therefore, we assume coherent reflection conditions, satellite elevation angles of  $3^\circ$  to  $30^\circ$  and layers of the different media (with their relative permittivity): dry snow cover ( $\sim 1$ ), low/high-salinity ice layer ( $\sim 3/\sim 5$ ) and underlying sea water ( $\sim 70$ ). Furthermore, we analyze reflectivity profiles estimated from GNSS reflectometry data of the first MOSAiC drift period (10/2019 to 06/2020) in the central Arctic. The comparison of model and estimation results shows that oscillation patterns occur when low permittivity coincides with low conductivity (low-salinity ice or dry snow). The patterns are particularly strong during post-warming period (PWP) in late April 2020 after three days of warm air intrusion at the ice floe. We conclude that structural changes of the sea-ice/snow layers upon temperature change can be detected by reflectometry measurements. Upcoming satellites (e.g. ESA's nano-satellite PRETTY) will provide further opportunities to study reflectometry data over sea ice in the Arctic and Antarctic.

## Data Acquisition and Processing

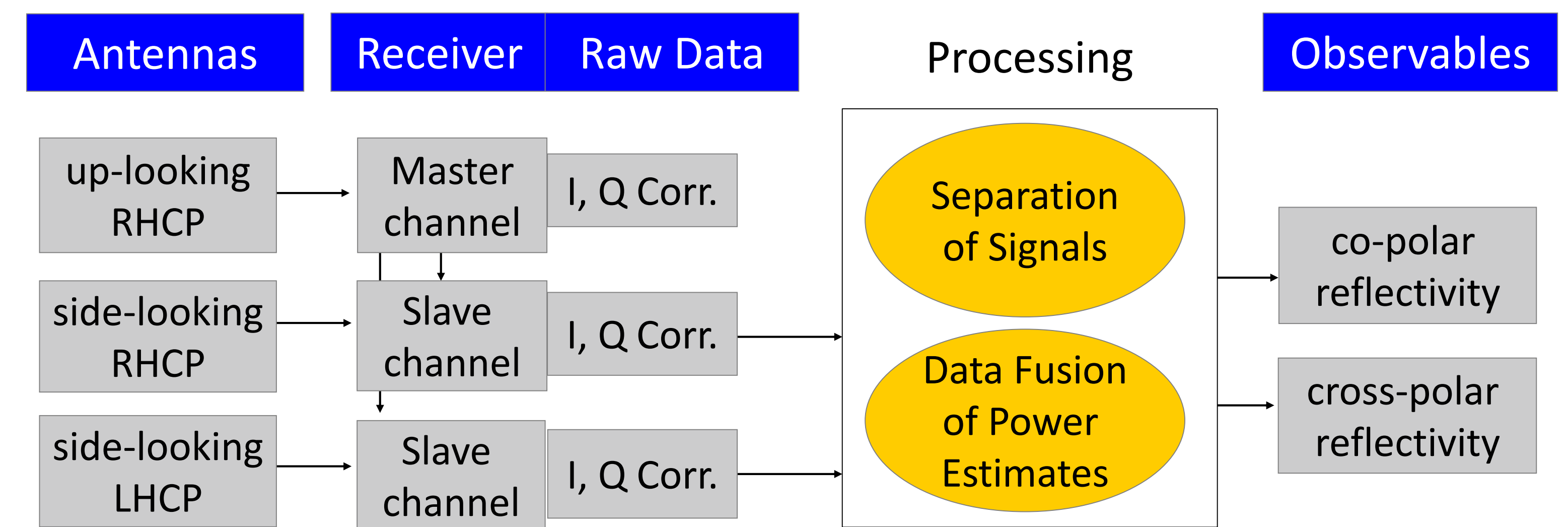


Fig. 4: Scheme of data acquisition and processing for reflectivity retrieval with the shipborne setup.

**Data Acquisition:** two antennas are used, the up-looking one dedicated to direct signals, the side-looking one to reflections in two polarizations right-handed (RHCP) and left-handed (LHCP). The up-looking link feeds Master channels, the side-looking links separated Slave channels. Each channel provides raw data of correlation samples with in-phase (I) and quadrature (Q) components. **Processing:** in a first step direct and reflected signals' contributions are separated and respective power is estimated from I,Q residuals. In a second (data fusion) step reflectivity is derived from power ratios: co-polar (RHCP reflected to RHCP direct) and cross-polar (LHCP reflected to RHCP direct). More details in [1], [3].

## GNSS Reflectometry and MOSAiC drift

Why GNSS signals?

- They give opportunity for remote sensing
- Reflected signals to sense Earth surface
- Systems with global coverage
- Rather inexpensive setup

Why MOSAiC?

- Observatory with various techniques drifting across the Arctic [1] where few data exist
- Reflectometry data recorded over long period
- Under changing, however, monitored conditions (air temperature, sea-ice concentration etc.)

Meaning of Reflectivity:

- Reflectivity is sensitive to sea-ice properties (e.g. sea-ice concentration) [2]
- it can be retrieved from ratio of reflected and direct signal power
- Can we model the estimated reflectivity and invert sea-ice properties (especially the ice type)?

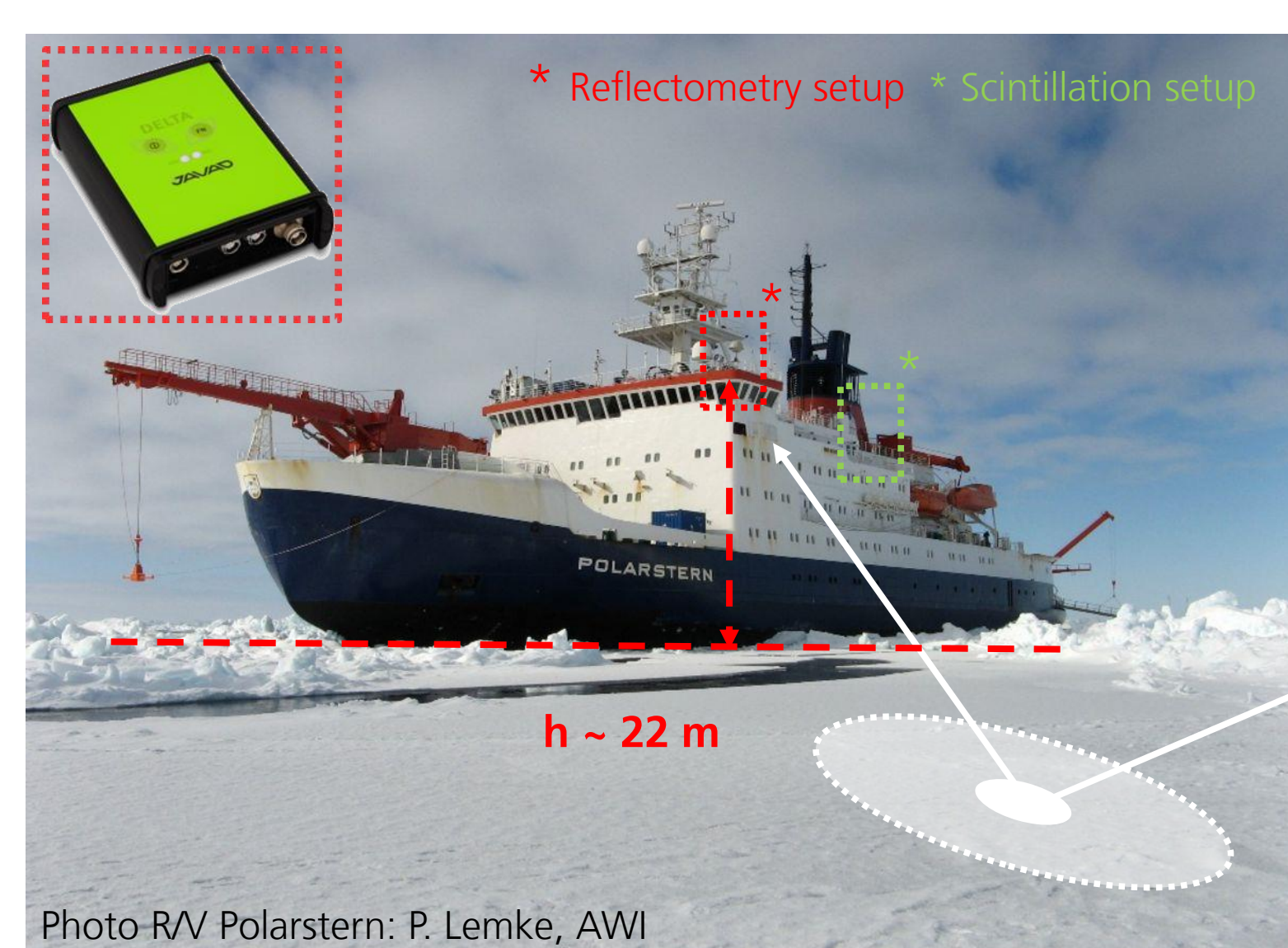


Photo-RV Polarstern: P. Lemke, AWI  
Fig. 1: Location of GNSS setups (reflectometry in red) installed for MOSAiC on RV Polarstern.

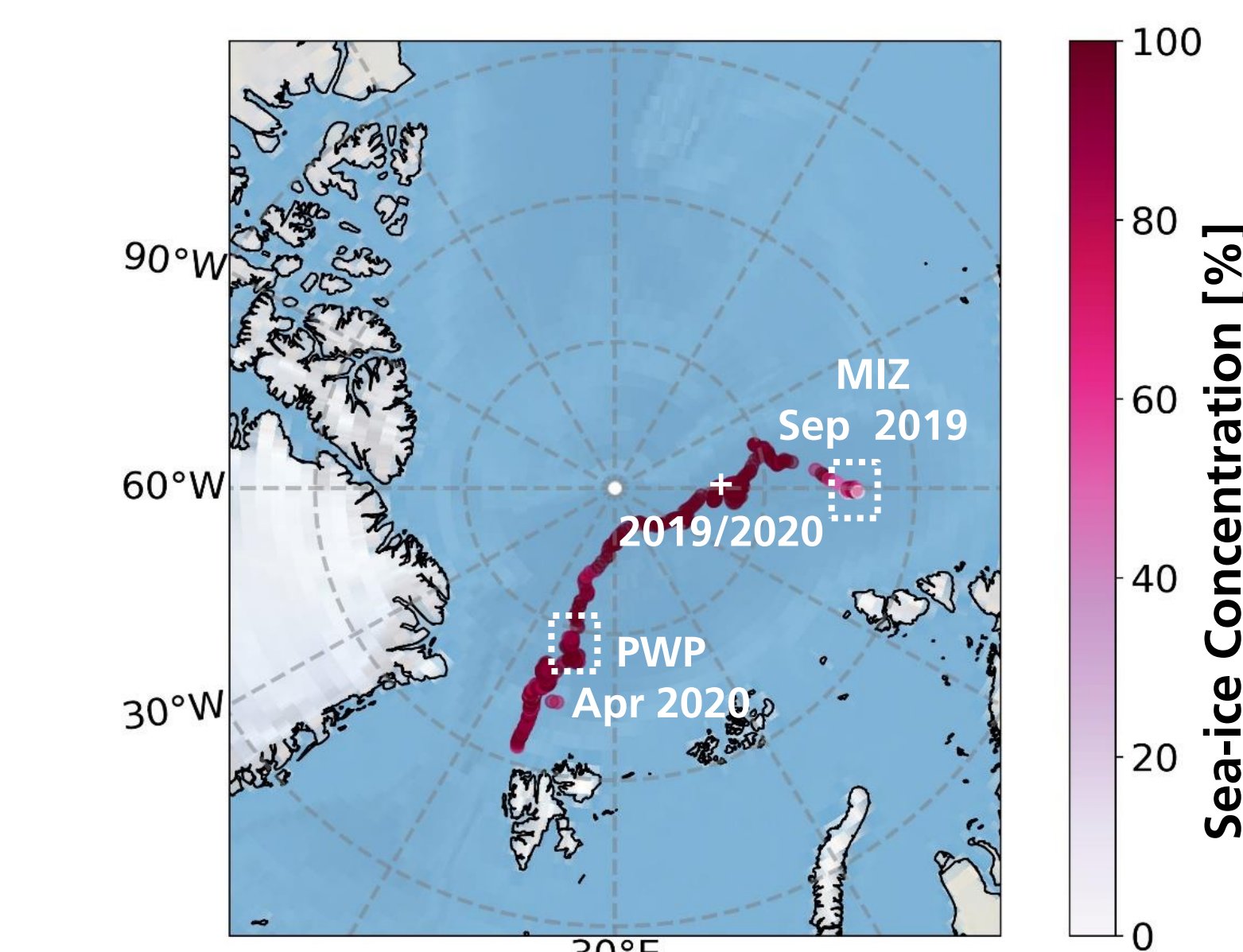


Fig. 2: Trajectory of R/V Polarstern during first drift Sep 2019 to Jun 2020, Marginal Ice Zone (MIZ) and Post-Warming Period (PWP) indicated.

## Multi-layer Reflectivity Model

**Background:** In contrast to a water surface the penetration of sea-ice by GNSS signals cannot be neglected. The concept of slab reflection has been used for sea-ice microwave radiometry [3]. It applies also, in an iterative way, to multi-layer reflectometry [4], [5].

**Components:** the scenario here considers an upper medium (air), two layers (snow, sea-ice) and lower medium (water). **Model Input:** rel. permittivity and conductivity of all media, thickness of layers and elevation angle at upper-most interface (air-snow).

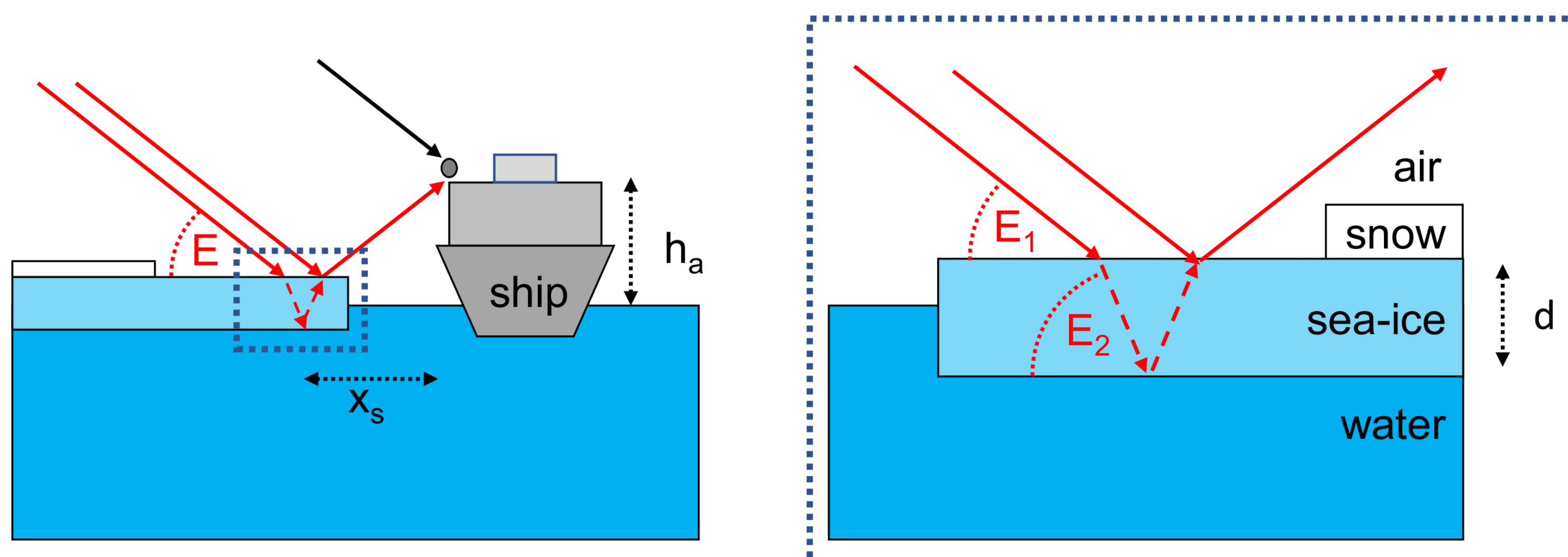


Fig. 3: Scheme of sea-ice reflection observed on a ship: reflected rays (red) and direct ray (black). The receiving antenna is located in a height  $h_a \sim 22\text{m}$  above the surface, reflection points appear typically in a distance  $x_s$  of 30 to 100m. **Zoom:** on reflections at air-ice and ice-water interface, the ice-penetrating rays (dashed red) are refracted. For simplicity snow is not considered. Adopted from [5].

## Modelling and Observation Results

**Reflectivity profiles:** The shipborne scene, cf. Fig. 1, allows an unrestricted view to port-side where the data record covers slant elevation angles ( $1^\circ$  to  $45^\circ$ ). Modelled and observed reflectivity profiles over this elevation range are presented in Fig. 5 and 6, respectively. **Model settings:** Fig. 5 shows co-polar profiles (left column), cross-polar profiles (center, right column). **Ice types** (sorted by rows): high-salinity first-year (FY) and low-salinity multiyear (MY) ice (upper and lower rows). **Number of layers** (indicated by line color and pattern): no layer just bulk reflection over water or ice (solid or dashed red lines), ice layer reflection (dashed black lines) and ice layer with covering snow layer (dotted black line). **Ice thickness** (indicated by line thickness): different curves in right column. **Observation settings:** Fig. 6 shows co- and cross-polar profiles (left and right column) during two observation period, cf. Fig 2: in the MIZ at the beginning of the drift (3 days in Sep 2019) and during the PWP late in the drift (second half of April 2020).

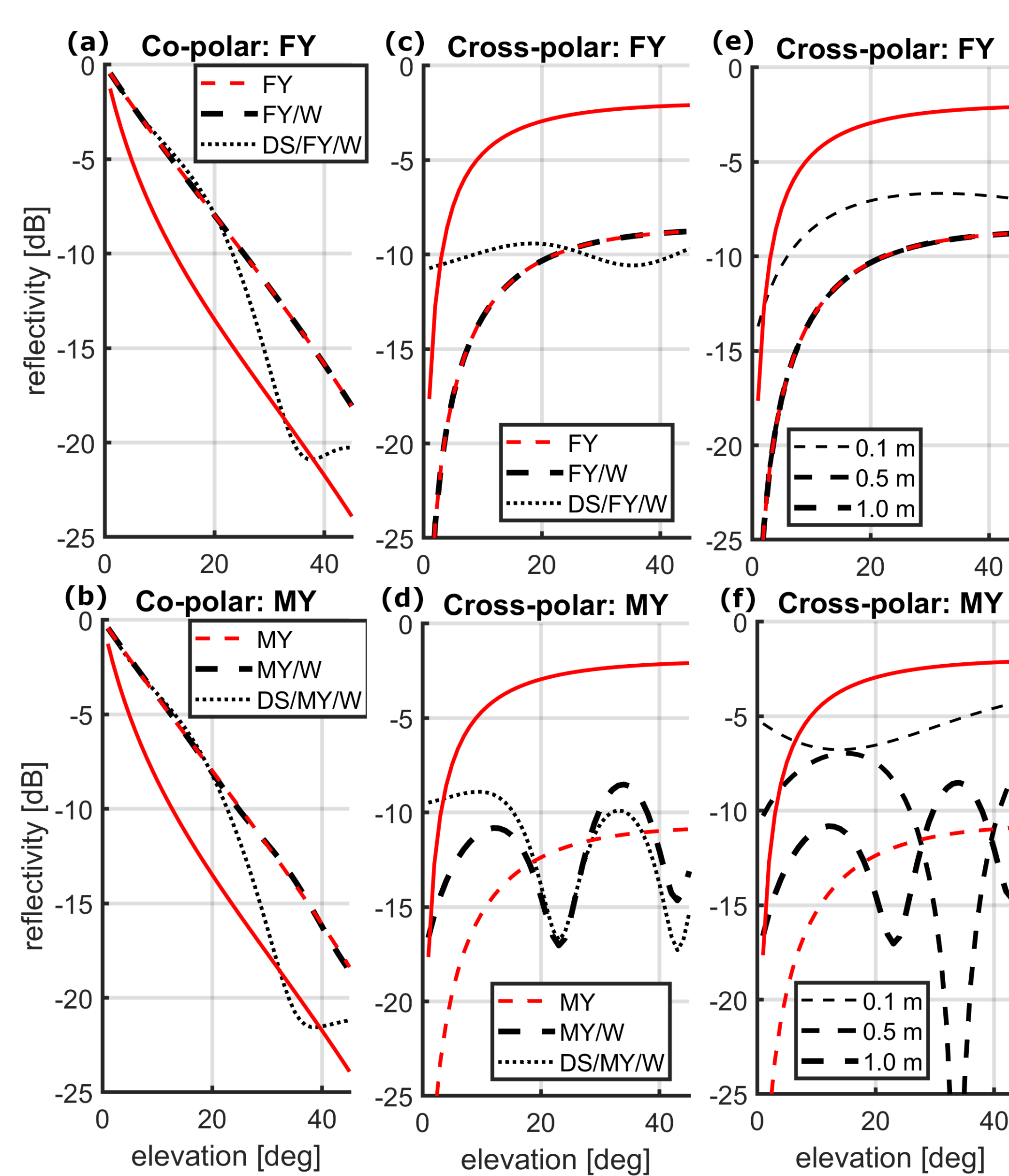


Fig. 5: Model results for different configurations. Adopted from [5].

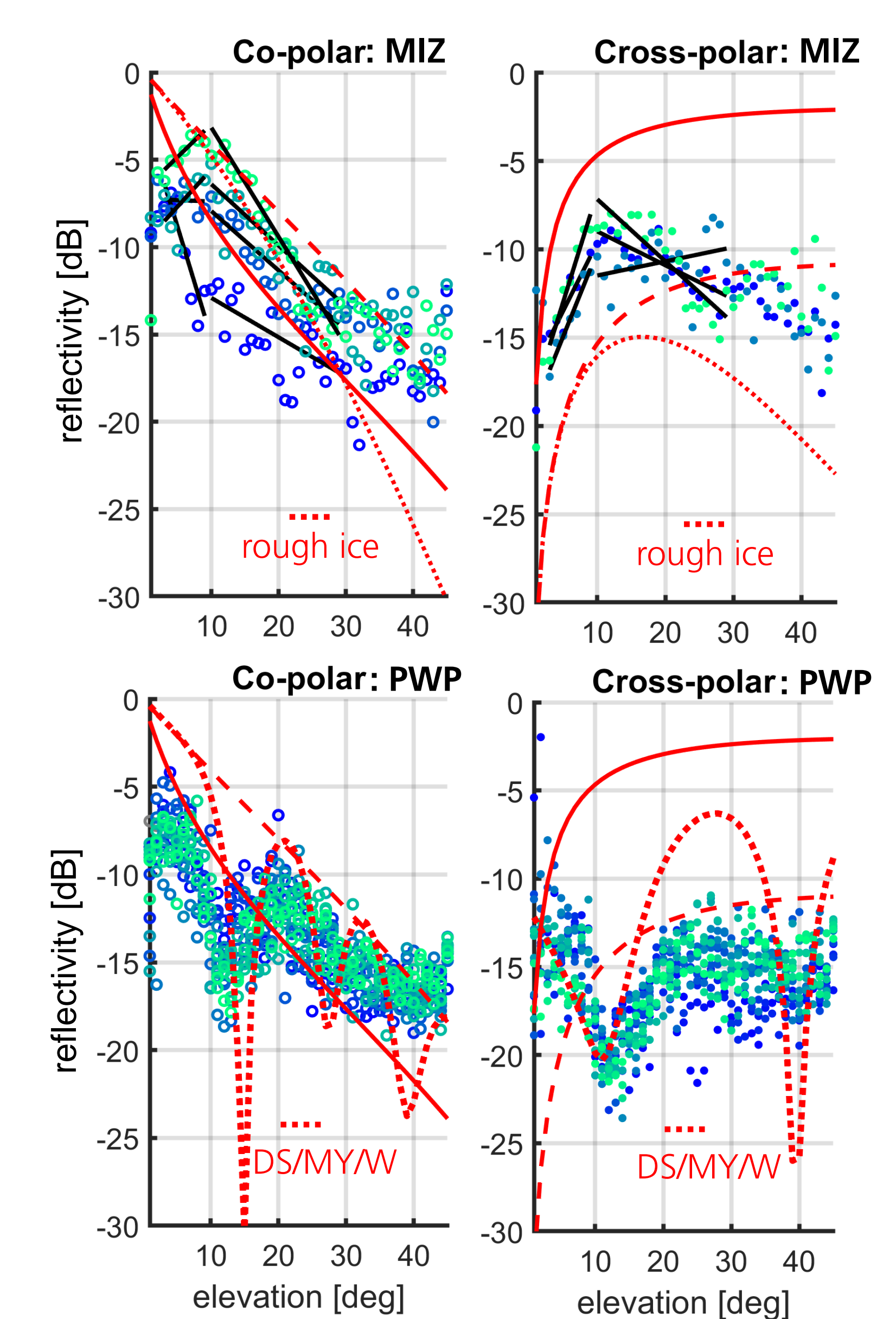


Fig. 6: Observation results during different periods.

## Discussion and Conclusions

**Model results:** Cross-polar profiles, in general, are more sensitive to changes in sea-ice properties than co-polar profiles (Fig. 5). The cross-polar profiles decrease in reflectivity level if the salinity of ice types decreases, compare bulk medium curves (red) for water, FY and MY ice. Changes in ice-layer thickness have almost no impact on profiles for high salinity ice (FY). Only for low-salinity ice (MY), when penetration occurs, anomalies (oscillation pattern) in cross-polar profiles are found. A loss-less cover (like dry snow) of the sea ice layer influence all scenarios, even co-polar and FY profiles change in the presence of a dry-snow layer.

**Observation results:** Cross-polar profiles from the MIZ in Fig. 6 (dots presenting color-coded daily mean blue to green) agree quite well with model prediction for bulk ice reflection damped by roughness (red dotted curve). Obvious oscillations deviating from the bulk ice prediction (with deep fades in the profile) occur in the PWP. Such oscillation patterns (in co- and cross-polar profiles) can be reproduced by the multi-layer model assuming low-salinity ice and a dry snow cover. Further retrieval of layer thicknesses requires to solve ambiguities in the oscillations [4]. **Conclusion:** a low-salinity ice type can be identified by an oscillation pattern in the profile. Changes in ice/snow type can be detected by analyzing the profiles.

## References

- [1] Nicolaus et al. [2022]: "Overview of the MOSAiC expedition: Snow and sea ice". Elem. Sci. Anth. 10 (1). doi: 10.1525/elementa.2021.000046
- [2] Semmling et al. [2019]: "Sea Ice concentration derived from GNSS reflection measurements in Fram Strait". IEEE Trans. Geosci. Rem. Sens. 57.12, pp. 10350–10361. doi: 10.1109/TGRS.2019.2933911
- [3] Kaleschke et al. [2010]: "A sea-ice thickness retrieval model for 1.4 GHz radiometry and application to airborne measurements over low salinity sea-ice". In: The Cryosphere 4, pp. 583–592.
- [4] Munoz-Martin et al. [2020]: "Snow and Ice Thickness Retrievals Using GNSS-R: Preliminary Results of the MOSAiC Expedition". Remote Sensing 12, p. 4038. doi: 10.3390/rs12244038.
- [5] Semmling et al. [2022]: "Sea-ice permittivity derived from GNSS reflection profiles: Results of the MOSAiC expedition". IEEE Trans. Geosci. Rem. Sens. 60, p. 4302416. doi: 10.1109/TGRS.2021.3121993.

Acknowledgments: We grateful for the efforts of the *Polarstern* crew and AWI's technical and logistical efforts. IT and Werkstatt services at GFZ and DLR are kindly acknowledged that were essential to prepare the GNSS setups and to transfer the data. Thanks to Lars Kaleschke, Robert Ricker and Aikaterini Tavri for their on-site support.

Contact: M. Semmling  
DLR, Institute for Solar-Terrestrial Physics  
Kalkhorstweg 53, 17235 Neustrelitz, Germany  
Email: maximilian.semmling@dlr.de